Solvatochromism of novel donor–π–acceptor type pyridinium dyes in halogenated and non-halogenated solvents

Yousuke Ooyama, Risa Asada, Shogo Inoue, Kenji Komaguchi, Ichiro Imae and Yutaka Harima*

Received (in Victoria, Australia) 14th July 2009, Accepted 18th August 2009
First published as an Advance Article on the web 17th September 2009
DOI: 10.1039/b9nj00332k

Donor–π–acceptor type pyridinium dyes that have been newly synthesized showed bathochromic shift of the absorption band with decreasing dielectric constant (ε_r) of solvent (negative solvatochromism), and the bathochromic shifts in halogenated solvents were larger than those in non-halogenated solvents of similar ε_r values. The influences of halogenated solvents on the large bathochromic shifts are studied on the basis of ^{1}H NMR measurements, semi-empirical molecular calculations (AM1 and INDO/S using the SCRF Onsager model), and absorption spectral measurements of the dyes adsorbed on nanocrystalline TiO_2 film immersed in solvents.

Introduction

Donor–π–acceptor (D–π–A) type pyridinium dyes with both electron-donating (D) and electron–accepting (A) groups linked by a π-conjugated bridge with intense absorptions, and electro-optic (EO) and nonlinear optical (NLO) properties have created considerable interest in recent years for their potential applications to optoelectronics and photonics such as photoelectric conversion systems and optical data processing and storage.[1–4] The D–π–A type pyridinium dyes are known well to show negative solvatochromism (*i.e.*, bathochromic shift of the absorption band with decreasing dielectric constant (ε_r) of solvent (solvent polarity)), which have been studied systematically by many researchers.[4–8] In the other words, with increasing solvent polarity, the absorption band shows a hypsochromic shift. It has been speculated from ^{1}H and ^{13}C NMR measurements and molecular orbital (MO) calculations that the negative solvatochromism would be ascribed to the change of the electronic ground-state structure of the pyridinium dye on changing of solvent polarity; with increasing solvent polarity the ground state is more stabilized than that of the excited state because the ground state is more dipolar than the excited state, and this produces a hypsochromic shift.[5,7] Another feature of the pyridinium dyes is that the bathochromic shifts in halogenated solvents such as dichloromethane and chloroform are larger than those in non-halogenated solvents of similar ε_r values such as toluene and hexane.[4–8] In particular, the D–π–A type pyridinium dyes with dialkylamine or diphenylamine moieties as electron donor and pyridinium ring as electron acceptor exhibit notable bathochromic shifts in halogenated solvents.[8] Up to the present time, however, there have been few efforts to clarity the influences of halogenated solvent on the large bathochromic shift, although the phenomenon is of a great interest form an academic viewpoint, together with a practical importance.

Department of Applied Chemistry, Graduate School of Engineering, Hiroshima University, Higashi-hiroshima 739-8527, Japan. E-mail: harima@mls.ias.hiroshima-u.ac.jp; Fax: +81 82-424-5494

In this paper, we describe the synthesis and the negative solvatochromic behaviors of novel D–π–A type pyridinium dyes (**4**) and (**5**) with a dibutylamino group and pyridinium ring linked by a π-conjugated bridge. In accordance with the previous reports, the bathochromic shifts of **4** and **5** in halogenated solvents are larger than those of the non-halogenated solvents of low ε_r values. The influences of halogenated solvents on the large bathochromic shifts are studied on the basis of ^{1}H NMR measurements, semi-empirical molecular calculations (AM1 and INDO/S using the SCRF Onsager model), and absorption spectral measurements of the dyes adsorbed on nanocrystalline TiO_2 film immersed in solvents.

Results and discussion

Synthesis of D–π–A type pyridinium dyes

The synthetic pathway of pyridinium dyes **4** and **5** is shown in Scheme 1. We used 3-dibutylamino-8*H*-5-oxa-8-aza-indeno-[2,1-*c*]fluorene-6,7-dione **1**[9] as a starting material. The quinone **1** was allowed to react with 4-pyridinecarbaldehyde to give the structural isomers **2** and **3** in 31 and 12% yields, respectively. The reaction of **2** or **3** with 1-iodobutane gave the pyridinium dyes **4** (93% yield) or **5** (91% yield).

Solvatochromic behaviors of D–π–A type pyridinium dyes

The solvatochromic spectral data of **4** and **5** are summarized in Table 1 and the spectra of **4** and **5** in various solvents are depicted in Fig. 1. The pyridinium dyes **4** and **5** show two absorption maxima: one band occurs at around 370 nm ascribed to π → π* transitions for both **4** and **5**, and another band occurs at around 540–640 nm for **4** and 420–500 nm for **5** assigned to intramolecular charge transfer (ICT) excitation from the dibutylamino group to the pyridinium ring. The ICT band of **4** occurs at a longer wavelength than that of **5**. On the other hand, the π → π* transition for **5** is stronger than that for **4**. These results suggest that an increase in the ICT characteristics leads to a decrease in π → π* transitions, so that the degree of donor–acceptor conjugation for **4** is larger

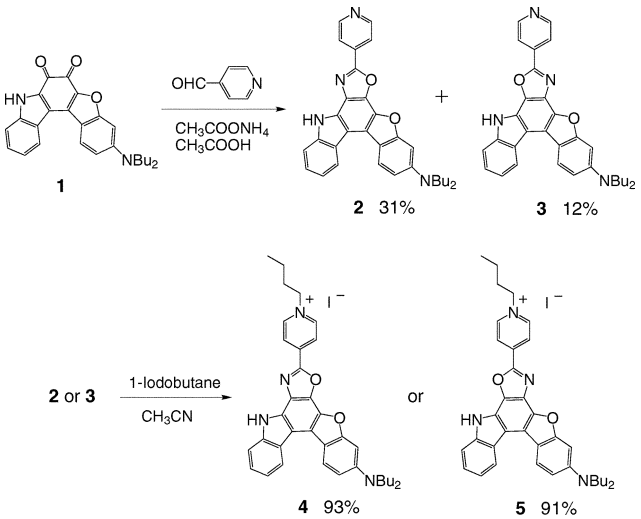

Scheme 1 Synthesis of pyridinium dyes **4** and **5**.

than that for **5** owing to the conjugated linkage of the dibutylamino group to the pyridinium ring in **4**. The ICT bands for both **4** and **5** exhibit a strong negative solvatochromism (Table 1). With decreasing solvent polarity from DMSO (ε_r = 47.24) to toluene (ε_r = 2.38), the ICT band of **4**, in particular, shifts from 534 to 595 nm. It is worthy to note here that the bathochromic shifts are prominent in halogenated solvents: the ICT bands of **4** in all the halogenated solvents appear at wavelengths longer than that of **4** in the least polar toluene. Furthermore, although the ε_r value of dibromomethane (ε_r = 7.77) is very close to that of tetrahydrofuran (ε_r = 7.52), the ICT band of **4** in dibromomethane occurs at 611 nm compared with 567 nm in tetrahydrofuran. Fig. 2 shows color changes of **4** in various solvents.

To elucidate the influences of solvent polarity on the ICT bands of **4**, semi-empirical MO calculations of **4** were carried out by the INDO/S method[11] using the SCRF Onsager model after geometrical optimizations using the MOPAC/AM1 method.[12] The calculated absorption data are collected in Table 2. For all the solvents used, the calculations show that the first excitation bands of **4** are mainly assigned to a transition from the HOMO to the LUMO, where HOMOs are mostly localized on the 3-dibutylaminobenzofuro[2,3-*c*]-oxazolo[4,5-*a*]carbazole moiety and LUMOs are mostly localized on the pyridinium moiety (Fig. 3(a)). The changes in the calculated electron density accompanying the first electron excitation are shown in Fig. 3(b), which reveals that the ICT occurs from the 3-dibutylaminobenzofuro[2,3-*c*]oxazolo[4,5-*a*]-carbazole moiety to the pyridinium moiety. The calculation demonstrates that with decreasing solvent polarity from DMSO to toluene the ICT bands show bathochromic shifts from 493 to 580 nm (Table 2). In order to see the influence of solvent polarity on the ICT bands more explicitly, the wavenumbers of the experimental and calculated absorption maxima for the ICT bands of **4** are plotted against the ε_r value of the solvent in Fig. 4. The plot of the calculated absorption maximum against ε_r shows that the wavenumber increases slightly with the increase in ε_r (Fig. 4(b)). On the other hand,

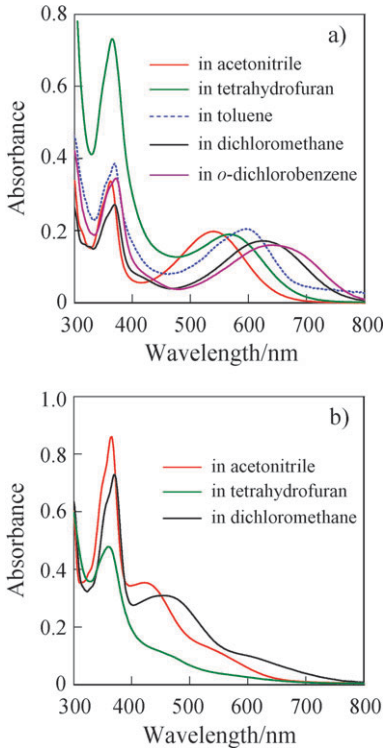

Fig. 1 Absorption spectra of (a) **4** and (b) **5** in different polar solvents. The absorption spectrum of **4** in toluene is enlarged because of poor solubility of **4**.

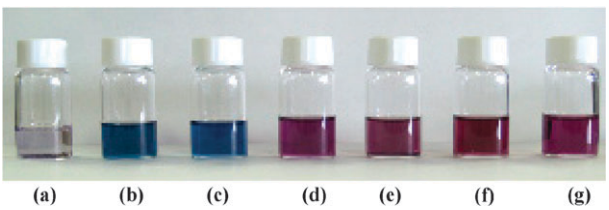

Fig. 2 Solvatochromic properties of **4** in various solvents: (a) toluene, (b) chloroform, (c) dichloromethane, (d) ethyl acetate, (e) tetrahydrofuran, (f) acetone, and (g) acetonitrile.

the plot of the experimental absorption maximum against ε_r differs considerably from that of the calculation (Fig. 4(a)). However, when the plots of halogenated solvents are excluded from the plot of Fig. 4(a), the plot of Fig. 4(a) shows a similar profile to that of Fig. 4(b).

The above comparison of the experimental and calculated absorption maxima hints that the interactions of halogenated solvent molecules with dye molecules contribute to the large bathochromic shifts of ICT band in halogenated solvents. Thus, we performed the absorption spectral measurements of **4** in mixed solvents of non-halogenated solvent (acetonitrile or THF) and halogenated solvent (chloroform or dibromomethane). We have plotted the wavenumber of the absorption maximum against the mixture composition. In all cases, the plots were almost linear, and we could not obtain useful information for specific interactions between the dye molecule and the halogenated or non-halogenated solvents.

Table 1 Solvatochromic spectral data of **4** and **5**[a]

Dye	No.	Solvent	ε_r[b]	λ_{max}^{abs}/nm (ε_{max}/M^{-1} cm^{-1})[c]
4	1	Toluene	2.38	595 (—)[d]
	2	Chloroform	4.81	610 (12000)
	3	Diiodomethane	5.32	634 (10900)
	4	Fluorobenzene	5.47	593 (—)[d]
	5	Ethyl acetate	6.09	546 (10100)
	6	Tetrahydorofuran	7.52	567 (9500)
	7	Dibromomethane	7.77	611 (7400)
	8	Dichloromethane	8.93	624 (8600)
	9	*o*-Dichlorobenzene	10.12	641 (8000)
	10	1,2-Dichloroethane	10.42	622 (16100)
	11	Acetone	21.10	542 (9800)
	12	Ethanol	25.3	564 (9600)
	13	Acetonitrile	36.64	540 (9900)
	14	Dimethyl sulfoxide	47.24	534 (8800)
5	5	Ethyl acetate	6.09	433 (5700)
	6	Tetrahydorofuran	7.52	450 (5700)
	8	Dichloromethane	8.93	455 (15500)
	11	Acetone	21.10	424 (19500)
	13	Acetonitrile	36.64	422 (17700)

[a] 2.0×10^{-5} M. [b] Dielectric constant (ref. 10). [c] The longest wavelength absorption maximum. [d] Poorly soluble.

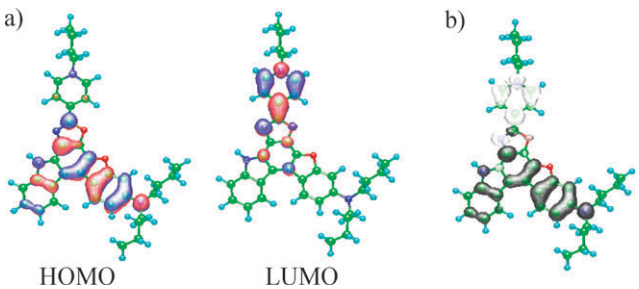

Fig. 3 (a) HOMO and LUMO electron densities of **4**. The red and blue lobes denote the positive and negative signs of the coefficients of the molecular orbitals. The size of each lobe is proportional to the MO coefficient. (b) Calculated electron density changes accompanying the first electronic excitation of **4**. The black and white lobes signify decrease and increase in electron density accompanying the electronic transition, respectively. Their areas indicate the magnitude of the electron density change (light blue, green, blue and red balls correspond to hydrogen, carbon, nitrogen and oxygen atoms, respectively.

^{1}H NMR measurements

The influence of solvent on the electronic ground-state structure of **4** was examined by the ^{1}H NMR measurements in DMSO-d_6 of a high ε_r value and THF-d_8 of a relatively low ε_r value as the non-halogenated solvents, and in CD_2Cl_2 and $CDCl_3$ as the halogenated solvents (Fig. 5). The chemical shifts of aromatic protons in CD_2Cl_2 are nearly the same as those in $CDCl_3$, and those in THF-d_8 show slightly upfield shifts compared to those in DMSO-d_6. Remarkable differences were observed between the halogenated and non-halogenated solvents: the chemical shifts of H2, H3, H4, H7, H8 and H11 show upfield shifts on changing solvents from DMSO-d_6 or THF-d_8 to CD_2Cl_2 or $CDCl_3$. Furthermore, the NH of carbazole ring varies from 12.67 ppm in DMSO-d_6 and 11.78 ppm in THF-d_8 to 9.83 ppm in CD_2Cl_2 and 9.43 ppm in $CDCl_3$. It is worth noting that the chemical shifts in CD_2Cl_2 show significantly upfield shifts compared to those in THF-d_8, although the ε_r value of CH_2Cl_2 is close to that of THF. It is apparent that the observed upfield shifts in the halogenated solvents are responsible for a shift of the electronic structure due to strong D–π–A interactions between the π-electron system of the chromophore containing pyridinium ring and the lone pairs of electrons on nitrogens of the dibutylamino group and the carbazole ring. Therefore, it is suggested that the ICT characteristics of **4** became stronger in the halogenated solvents.

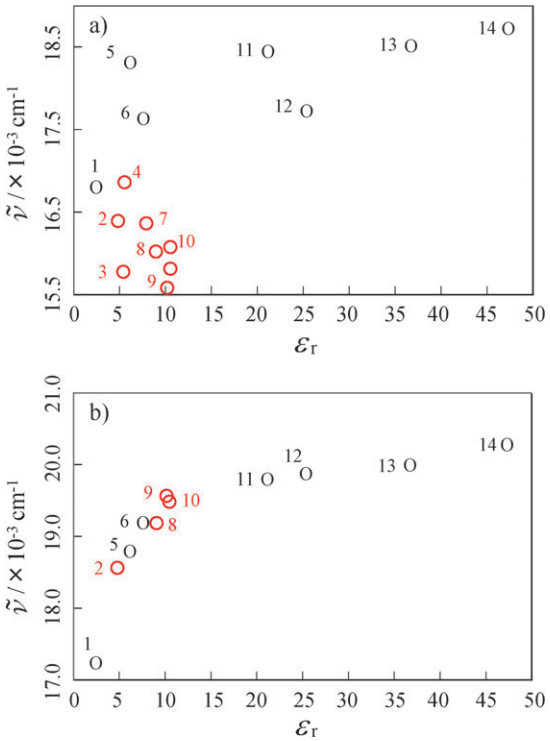

Fig. 4 Wavenumber ($\tilde{\nu}$) of (a) the experimental and (b) calculated absorption maximum for the ICT bands of **4** *vs.* dielectric constant (ε_r) of the solvent. The numbers correspond to those of Table 1 and Table 2, respectively. The circles in red show halogenated solvents.

Table 2 Calculated absorption spectra for **4**

Solvent	No.	Absorption λ_{max}/nm	f[a]	CI component[b]
Toluene	1	580	1.00	HOMO → LUMO (84%)
Chloroform	2	539	0.97	HOMO → LUMO (84%)
Ethyl acetate	5	532	0.96	HOMO → LUMO (84%)
Tetrahydrofuran	6	521	0.96	HOMO → LUMO (84%)
Dichloromethane	8	521	0.96	HOMO → LUMO (84%)
o-Dichlorobenzene	9	511	0.97	HOMO → LUMO (84%)
1,2-Dichloroethane	10	513	0.96	HOMO → LUMO (84%)
Acetone	11	505	0.95	HOMO → LUMO (85%)
Ethanol	12	503	0.95	HOMO → LUMO (85%)
Acetonitrile	13	500	0.95	HOMO → LUMO (85%)
Dimethyl sulfoxide	14	493	0.96	HOMO → LUMO (85%)

[a] Oscillator strength. [b] The transition is shown by an arrow from one orbital to another, followed by its percentage CI (configuration interaction) component.

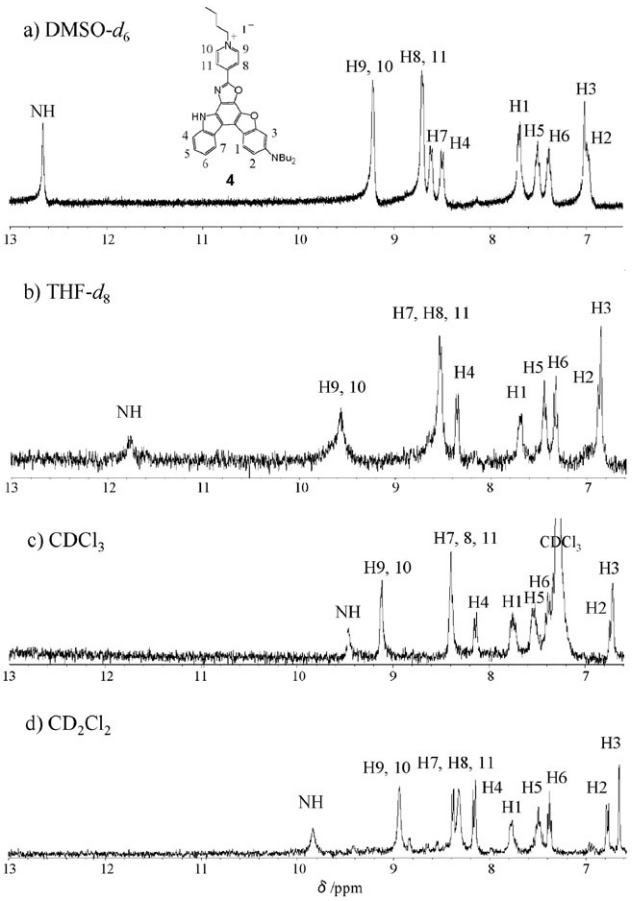

Fig. 5 ^{1}H NMR spectra of **4** in (a) DMSO-d_6 (b) THF-d_8, (c) $CDCl_3$ and (d) CD_2Cl_2.

Absorption spectral measurements of the dyes adsorbed on nanocrystalline TiO_2 films immersed in solvents

To gain a further insight into the influences of halogenated solvents on the ICT characteristics, we performed the absorption spectral measurements of **4** adsorbed on nanocrystalline TiO_2 film immersed in solvents (see Experimental section for preparation of the nanocrystalline TiO_2 film). If the solvent molecules affect directly the electronic structure of **4**, the ICT bands should be shifted. As shown in Fig. 6, the ICT band of **4** adsorbed on TiO_2 film in air (no solvent) is observed at 570 nm. The ICT bands (570–580 nm) of **4** adsorbed on TiO_2 film immersed in toluene and ethyl acetate appears in almost the same wavelength region as that in air, so that the ICT bands of **4** adsorbed on TiO_2 film were not affected by toluene and ethyl acetate. On the other hand, the ICT band (610 nm) of **4** adsorbed on TiO_2 film immersed in chloroform or dichloromethane is red-shifted by 30–40 nm compared to that immersed in toluene and ethyl acetate. The absorption spectra of **4** adsorbed on TiO_2 films immersed in acetone, acetonitrile and dimethyl sulfoxide were not obtained, because in those solvents, unfortunately, dye **4** was desorbed from the TiO_2 surface. On the basis of these results, as shown in Fig. 7, it was considered that the dye **4** is adsorbed on the TiO_2 film by an electrostatic interaction between the pyridinium moiety of **4** and the hydroxy group of the TiO_2 surface, and that the

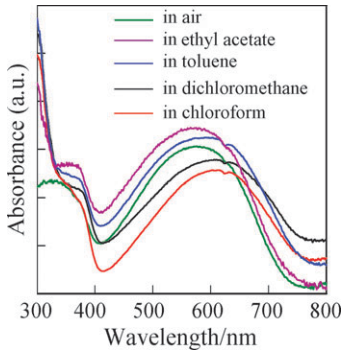

Fig. 6 Absorption spectra of **4** adsorbed on nanocrystalline TiO_2 films in air and immersed in solvents.

dibutylamino group and carbazole moiety of **4** interact with halogenated solvents. These suggest that halogenated solvents affected mainly the electron-donating property of **4**, leading to a higher HOMO energy level. Thus, the above results demonstrate that the enhancement of the D–π–A interactions is induced by halogenated molecules, which leads to stronger ICT characteristics responsible for the large bathochromic shifts of ICT bands.

Conclusions

In conclusion, novel donor–π–acceptor type pyridinium dyes **4** and **5** have been synthesized and their solvatochromic properties were investigated. The pyridinium dyes exhibited negative solvatochromism with unusual bathochromic shifts of the ICT band of **4** in halogenated solvents. Based on the ^{1}H NMR measurements in the halogenated and non-halogenated solvents and the absorption spectral measurements of pyridinium dye adsorbed on nanocrystalline TiO_2 film immersed in solvents, we have demonstrated that the D–π–A interactions are enhanced in halogenated solvents, which is responsible for the large bathochromic shifts of the ICT bands. Further studies on the solvatochromism for the donor–π–acceptor type pyridinium dyes are now in progress to account for the influences of the electronic structures of the pyridinium dyes on the large bathochromic shifts of the ICT bands in halogenated solvents.

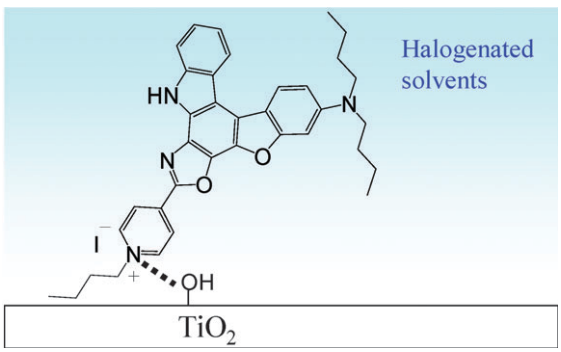

Fig. 7 Plausible configuration of **4** adsorbed on nanocrystalline TiO_2 films immersed in halogenated solvents.

Experimental

Melting points were measured with a Yanaco micro melting point apparatus MP model. IR spectra were recorded on a Perkin Elmer Spectrum One FT-IR spectrometer by ATR method. Absorption spectra were observed with a Shimadzu UV-3150 spectrophotometer. The nanocrystalline TiO_2 film were prepared as follows. To powdered TiO_2 (P-25, d = 30–40 nm, 1.30 g) in a mortar was added water (1.9 mL) in six portions with good stirring. Then, three drops of 12 M nitric acid and polyethylene glycol (80 mg) were successively added, and the mixture was well kneaded to a smooth paste. It was then applied on a glass substrate and sintered for 30 min at 500 °C. Absorption spectra of the dyes adsorbed on TiO_2 film were measured in the diffuse-reflection mode by a Shimadzu UV-3150 spectrophotometer with a calibrated integrating sphere system ISR-3100. ^{1}H NMR spectra were recorded on a JNM-LA-400 (400 MHz) FT NMR spectrometer with tetramethylsilane (TMS) as an internal standard. Mass spectral data were acquired on a JEOL double-focusing mass spectrometer SX102A equipped with a FAB inlet system. Column chromatography was performed on silica gel (Kanto Chemical, 60N, spherical, neutral).

Preparation of 7-(4-pyridyl)-3-dibutylaminobenzofuro-[2,3-*c*]oxazolo[4,5-*a*]carbazole (2) and 7-(4-pyridyl)-3-dibutylaminobenzofuro[2,3-*c*]oxazolo[5,4-*a*]carbazole (3)

A solution of **1** (0.20 g, 0.48 mmol), *p*-cyanobenzaldehyde (0.052 g, 0.48 mmol) and ammonium acetate (0.75 g, 9.73 mmol) in acetic acid (50 ml) was stirred at 90 °C for 2 h. After concentrating under reduced pressure, the resulting residue was chromatographed on silica gel (toluene–acetic acid = 5 : 1 as eluent) to give **2** (0.074 g, yield 31%) as an orange powder and **3** (0.031 g, yield 12%) as an orange powder; **2**: mp 256–258 °C; IR (ATR): $\tilde{\nu}$ = 3061, 1624, 1602 cm^{-1}; ^{1}H NMR (acetone-d_6, TMS) δ = 1.03 (6H, t), 1.46–1.51 (4H, m), 1.70–1.76 (4H, m), 3.54 (4H, t), 7.04 (1H, dd, J = 1.96 and 8.00 Hz), 7.07 (1H, d, J = 1.96 Hz), 7.42 (1H, t), 7.53 (1H, t), 7.82 (1H, d, J = 8.00 Hz), 8.23 (2H, d, J = 6.80 Hz), 8.58 (1H, d, J = 8.00 Hz), 8.74 (1H, d, J = 8.00 Hz), 8.90 (2H, d, J = 6.80 Hz), 11.55 (1H, s, –NH); FABMS m/z 503 (M$^+$); **3**: mp 264–266 °C; IR (ATR): $\tilde{\nu}$ = 3095, 1602, 1559 cm^{-1}; ^{1}H NMR (DMSO-d_6, TMS) δ = 1.00 (6H, t), 1.39–1.46 (4H, m), 1.60–1.67 (4H, m), 3.20–3.48 (m, 4H) (overlap with peak of dissolved water in DMSO-d_6), 6.96 (2H, dd, J = 2.20 and 8.00 Hz), 7.09 (1H, d, J = 2.20 Hz), 7.43 (1H, t), 7.54 (1H, t), 7.73 (1H, d, J = 8.00 Hz), 8.20 (2H, d), 8.48 (1H, d, J = 8.80 Hz), 8.66 (1H, d, J = 8.80 Hz), 8.93 (2H, d), 11.55 (1H, s, –NH); FABMS m/z 503 (M$^+$).

Preparation of 4-(3-dibutylaminobenzofuro[2,3-*c*]oxazolo-[4,5-*a*]carbazol-7-yl)-1-butylpyridinium iodide (4)

A solution of **2** (0.04 g, 0.08 mmol) and iodobutane (100 mg) in dry acetonitrile (20 ml) was stirred at 80 °C for 24 h. After concentrating under reduced pressure, the resulting residue was subjected to reprecipitation from CH_2Cl_2–hexane to give **4** (0.041 g, yield 93%) as a dark purple solid; mp 271–273 °C; IR (ATR): $\tilde{\nu}$ = 3199, 1621 cm^{-1}; ^{1}H NMR (DMSO-d_6, TMS) δ = 0.85 (3H, t), 0.96 (6H, t), 1.20–1.25 (2H, m), 1.34–1.40 (4H, m), 1.59–1.62 (4H, m), 1.93–1.97 (2H, m), 3.20–3.60 (m, 4H) (overlap with peak of dissolved water in DMSO-d_6), 4.67 (2H, t), 6.97 (1H, d), 6.92 (1H, d), 7.39 (1H, t), 7.51 (1H, t), 7.69 (1H, d), 8.51 (1H, d), 8.62 (1H, d), 8.71 (1H, d), 9.23 (1H, d), 12.67 (1H, s, –NH); FABMS m/z 559 (M − I)$^+$.

Preparation of 4-(3-dibutylaminobenzofuro[2,3-*c*]oxazolo-[5,4-*a*]carbazol-7-yl)-1-butylpyridinium iodide (5)

A solution of **3** (0.065 g, 0.13 mmol) and iodobutane (100 mg) in dry acetonitrile (30 ml) was stirred at 80 °C for 17 h. After concentrating under reduced pressure, the resulting residue was subjected to reprecipitation from CH_2Cl_2–hexane to give **5** (0.066 g, yield 91%) as a dark brown solid; mp 270–273 °C; IR (ATR): $\tilde{\nu}$ = 3179, 1632 cm^{-1}; ^{1}H NMR (DMSO-d_6, TMS) δ = 0.87 (3H, t), 0.99 (6H, t), 1.23–1.25 (2H, m), 1.35–1.45 (4H, m), 1.60–1.65 (4H, m), 1.97–2.01 (2H, m), 3.25–3.58 (m, 4H) (overlap with peak of dissolved water in DMSO-d_6), 4.67 (2H, t), 6.96 (1H, d), 7.07 (1H, d), 7.40 (1H, t), 7.55 (1H, t), 7.74 (1H, d), 8.48 (1H, d), 8.66 (1H, d), 8.76 (1H, d), 9.29 (1H, d), 12.62 (1H, s, –NH); FABMS m/z 559 (M − I)$^+$.

Computational methods

The semi-empirical calculations were carried out with the WinMOPAC Ver. 3.9 package (Fujitsu, Chiba, Japan). Geometry calculations in the ground state were made using the AM1 method.[12] All geometries were completely optimized (keyword PRECISE) by the eigenvector following routine (keyword EF). Experimental absorption spectra of the four compounds were compared with their absorption data by the semi-empirical method INDO/S (intermediate neglect of differential overlap/spectroscopic)[11] using the SCRF Onsager Model. All INDO/S calculations were performed using single excitation full SCF/CI (self-consistent field/configuration interaction), which includes the configuration with one electron excited from any occupied orbital to any unoccupied orbital, where 225 configurations were considered [keyword CI (15 15)].

Acknowledgements

This work was supported by Grants-in-Aid for Scientific Research (B) (19350094) and for Young Scientist (B) (20750161) from the Japan Society for the Promotion of Science (JSPS), and by the Mazda Foundation.

References

1 (*a*) S. R. Marder, J. W. Perry and W. P. Schaefer, *Science*, 1989, **245**, 626; (*b*) R. Steinhoff, L. F. Chi, G. Marowsky and D. Möbius, *J. Opt. Soc. Am. B*, 1989, **6**, 843; (*c*) X. Liu, L. Liu, Z. Chen, X. Lu, J. Zheng and W. Wang, *Thin Solid Films*, 1992, **219**, 221; (*d*) S. R. Marder, J. W. Perry and C. P. Yakymyshyn, *Chem. Mater.*, 1994, **6**, 1137; (*e*) I. D. L. Albert, T. J. Marks and M. A. Ratner, *J. Phys. Chem.*, 1996, **100**, 9714; (*f*) X. Duan, H. Konami, S. Okada, H. Oikawa, H. Matsuda and H. Nakanishi, *J. Phys. Chem.*, 1996, **100**, 17780; (*g*) Y. Niidome, H. Ayukawa and S. Yamada, *J. Photochem. Photobiol., A*, 2000, **132**, 75; (*h*) B. J. Coe, J. A. Harris, I. Asselberghs, K. Wostyn, K. Clays, A. Persoons, B. S. Brunschwing, S. J. Coles, T. Gelbrich, M. E. Light, M. B. Hursthouse and K. Nakatani, *Adv. Funct. Mater.*, 2003, **13**, 347; (*i*) M. S. Chandra, Y. Ogata, J. Kawamata and T. P. Radhakrishnan, *Langmuir*, 2003, **19**, 10124; (*j*) H. Kang,

A. Facchetti, P. Zhu, H. Jiang, Y. Yang, E. Cariani, S. Righetto, R. Ugo, C. Zuccaccia, A. Macchioni, C. L. Stern, Z. Liu, S.-T. Ho and T. J. Marks, *Angew. Chem., Int. Ed.*, 2005, **44**, 7922.

2 (*a*) F. Pan, G. Knöpfle, Ch. Bosshard, S. Follonier, R. Spreiter, M. S. Wong and P. Günter, *Appl. Phys. Lett.*, 1996, **69**, 13; (*b*) U. Meier, M. Bösch, Ch. Bosshard, F. Pan and P. Günter, *J. Appl. Phys.*, 1998, **83**, 3486; (*c*) M. Thakur, J. J. Xu, A. Bhowmik and L. G. Zhou, *Appl. Phys. Lett.*, 1999, **74**, 635; (*d*) A. K. Bhowmik, S. Tan, A. C. Ahyi, A. Mishra and M. Thakur, *Polym. Mater. Sci. Eng.*, 2000, **83**, 169; (*e*) T. Kaino, B. Cai and K. Takayama, *Adv. Funct. Mater.*, 2002, **12**, 599.

3 (*a*) A.-D. Lang, J. Zhai, C.-H. Huang, L.-B. Gan, Y.-L. Zhao, D.-J. Zhou and Z.-D. Chen, *J. Phys. Chem. B*, 1998, **102**, 1424; (*b*) Z.-S. Wang, F.-Y. Li, C.-H. Huang, L. Wang, M. Wei, L.-P. Jin and N.-Q. Li, *J. Phys. Chem. B*, 2000, **104**, 9676; (*c*) F.-Y. Li, L.-P. Jin, C.-H. Huang, J. Zheng, J.-Q. Guo, X.-S. Zhao and T.-T. Liu, *Chem. Mater.*, 2001, **13**, 192.

4 (*a*) A. A. Turshatov, D. Möbius, M. L. Bossi, S. W. Hell, A. I. Vedernikov, N. A. Lobova, S. P. Gromov, M. V. Alfimov and S.Y. Zaitsev, *Langmuir*, 2006, **22**, 1571; (*b*) B. J. Coe, J. A. Harris, J. J. Hall, B. S. Brunschwig, S.-T. Hung, W. Libaers, K. Clay, S. J. Coles, P. N. Horton, M. E. Light, M. B. Hursthouse, J. Garín and J. Orduna, *Chem. Mater.*, 2006, **18**, 5907.

5 C. Reichardt, *Solvents and Solvent Effects in Organic Chemistry*, Wiley-VCH, Weinheim, 2003.

6 (*a*) P. Jacques, *J. Phys. Chem.*, 1986, **90**, 5535; (*b*) G. L. Gaines, Jr., *Angew. Chem., Int. Ed. Engl.*, 1987, **26**, 341; (*c*) F. M. Testoni, E. A. Riberio, L. A. Giusti and V. G. Machado, *Spectrochim. Acta, Part A*, 2009, **71**, 1704.

7 (*a*) A. Botrel, A. Beuze, P. Jacques and H. Strub, *J. Chem. Soc., Faraday Trans. 2*, 1984, **80**, 1235; (*b*) J. O. Morley, R. M. Morley, R. Docherty and M. H. Charlton, *J. Am. Chem. Soc.*, 1997, **119**, 10192.

8 (*a*) Y. Huang, T. Cheng, F. Li, C. Luo, C. H. Huang, Z. Cai, X. Zeng and J. Zhon, *J. Phys. Chem. B*, 2002, **106**, 10031; (*b*) M. Panigrahi, S. Dash, S. Patel, P. K. Behera and B. K. Mishra, *Spectrochim. Acta, Part A*, 2007, **68**, 757; (*c*) F. Dumur, C. R. Mayer, E. Dumas, F. Miomandre, M. Frigoil and F. Sécheresse, *Org. Lett.*, 2008, **10**, 321; (*d*) S. T. Abdel-Halim and M. K. Awad, *J. Mol. Struct.*, 2009, **920**, 332.

9 (*a*) Y. Ooyama and Y. Harima, *Chem. Lett.*, 2006, **35**, 902; (*b*) Y. Ooyama, Y. Kagawa and Y. Harima, *Eur. J. Org. Chem.*, 2007, 3613.

10 *CRC Handbook of Chemistry and Physics*, ed. D. R. Lide, CRC, Boca Raton, FL, 83rd edn, 2002.

11 (*a*) J. E. Ridley and M. C. Zerner, *Theor. Chim. Acta*, 1973, **32**, 111; (*b*) J. E. Ridley and M. C. Zerner, *Theor. Chim. Acta*, 1976, **42**, 223; (*c*) A. D. Bacon and M. C. Zerner, *Theor. Chim. Acta*, 1979, **53**, 21.

12 M. J. S. Dewar, E. G. Zoebisch, E. F. Healy and J. J. P. Stewart, *J. Am. Chem. Soc.*, 1985, **107**, 3902.

